CHEMICAL ENGINEERING TRANSACTIONS
VOL. 127, 2026
A publication of AIDIC
The Italian Association of Chemical Engineering
Online at www.cetjournal.it
Guest Editors: Laura Capelli, Marzio Invernizzi, Selena Sironi

ISBN 979-12-81206-28-1; **ISSN** 2283-9216
DOI: 10.3303/CET26127050

Kinetic Modelling of Microbial Au (III) Reduction by an Indigenous Bacterial Consortium

Miranda Mpeta*, Job T. Tendenedzai, Lehlogonolo Tabana, Shepherd Tichapondwa, Evans Chirwa

Water Utilization and Environmental Engineering Division, Department of Chemical Engineering, University of Pretoria, 0002.
u24054276@tuks.co.za

Gold mining effluents containing toxic Au (III) ions (typically 3–6 mg/L) present significant environmental and health risks. Conventional chemical recovery methods remain energy-intensive and generate secondary waste. This study developed and validated predictive kinetic models for microbial gold reduction using a specialized bacterial consortium. The consortium isolated from gold mine tailings comprised of *Stenotrophomonas maltophilia, Klebsiella pneumoniae, Acinetobacter bereziniae,* and *Bacillus cereus*. Aerobic batch bioreactors operating at 35°C compared synthetic wastewater (mineral salt medium (MSM) with $HAuCl_4$ at different concentrations of 1.5, 3 and 6 mg/L. Au (III) depletion was quantified by ICP-OES and AAS, while Au (0) nanoparticle formation was verified via X- ray diffraction (XRD), Scanning Electron Microscopy (SEM) with Energy-Dispersive X-ray Spectroscopy (EDS) and Transmission Electron Microscopy (TEM), revealing predominantly spherical particles (15–70 nm). The bacterial consortium achieved 87-99 % Au (III) reduction in synthetic wastewater within 24 h. Experimental data were fitted to a pseudo-first-order model using AQUASIM software ($0.726 > R^2 > 0.97$), providing a predictive description of Au (III) depletion in environmentally relevant concentrations.

1. Introduction

Gold mining tailings and wastewaters contain appreciable levels of Au (III) (often 1–6 mg/L) alongside other heavy metals, posing ecological and health hazards. Conventional recovery such as cyanide or thiourea leaching are costly, energy-intensive, and produces toxic by-products and large solid wastes (Malarkodi *et al.*, 2013). In contrast, microbial bioreduction of Au (III) to metallic gold (Au (0)) enables simultaneous detoxification and metal recovery under mild conditions. Various microbes are known to reduce Au (III) using different mechanisms. Bacteria can rapidly produce ~40 nm-150nm AuNPs via an NADPH-dependent reductase (Huang *et al*., 2005; Luo *et al*., 2015; Mpeta *et al*., 2025). *Cupriavidus metallidurans* utilizes a GolR enzyme to convert Au (III) into intracellular Au (0) nanoparticles (Wiesemann *et al*., 2017). Biogenic gold nanoparticles (AuNP) formation is documented in diverse microbes (bacteria, fungi, algae), often involving enzymatic electron transfers and intracellular nucleation (Abd El-Aziz *et al*., 2007; Lengke *et al*., 2007; Mata *et al*., 2009). Understanding the kinetics of microbial Au (III) bioreduction is critical for translating laboratory findings into practical engineered systems for wastewater treatment and metal recovery. Kinetic modelling provides quantitative insights into reaction rates, substrate dependencies, and optimal operational parameters, enabling the design of efficient bioreactors and prediction of system performance under varying environmental conditions (Igboamalu and Chirwa, 2016). Despite the growing body of research on microbial gold reduction mechanisms, there remains a significant gap in comprehensive kinetic characterization of these bioprocesses, particularly for mixed consortia operating across environmentally relevant concentration ranges (Jin, 2023; Guo and Wang, 2025). Mathematical models such as pseudo-first-order kinetics and Monod-type substrate inhibition models have proven valuable in describing microbial metal reduction systems, yet their application to Au (III) bioreduction by bacterial consortia remains limited (Wang *et al*., 2022). By developing kinetic models using AQUASIM software, this study aims to bridge the gap between mechanistic understanding and practical

Paper Received: 21 April 2026; Revised: 25 June 2026; Accepted: 8 July 2026
Please cite this article as: Mpeta M., Tendenedzai J.T., Tabana L., Tichapondwa S., Chirwa E., 2026, Kinetic Modelling of Microbial Au (III) Reduction by an Indigenous Bacterial Consortium, Chemical Engineering Transactions, 127, 295-300 DOI:10.3303/CET26127050

application. This helps provide a strong framework for scaling up microbial gold recovery technologies and optimizing process parameters for maximum efficiency and economic viability in real-world mining and industrial wastewater treatment scenarios. This study makes use of a mixed consortium due to the synergistic interactions and metabolic complementarity of the different strains for gold (III) reduction. The consortium showed ~95% reduction, likely via resource partitioning and metabolite exchange (Mpeta *et al.*, 2025). However, these prior results did not address kinetic modelling. This work extends those findings by (i) testing Au (III) bioreduction in defined Au (III) medium varying concentrations; (ii) developing kinetic models (pseudo-first-order, Monod) using AQUASIM software.

2. Materials and Methods

2.1 Bacterial isolation, culturing and storage

Four strains were isolated from gold tailings samples collected from a mine in Zimbabwe. The cultivation and storage procedure entailed cultivating the consortium in Tryptone Soy Broth (TSB) for 24 h at 35 °C on a rotary shaker at 100 rpm (FSIM-SPO8, Labcon, Johannesburg, South Africa). After 24 h, 0.8 mL of the TSB containing the bacteria was placed in sterilised 2 mL vials before adding 0.2 mL of 50% glycerol solution. Thereafter, the vials were placed in the −80 °C freezer for future use. The bacteria were streaked on agar plates and sent to Inqaba Biotechnical Industries (Pty) Ltd. (Pretoria, South Africa) for analysis. Bacteria were identified by 16S rRNA gene sequencing as *Stenotrophomonas maltophilia, Klebsiella pneumoniae, Acinetobacter bereziniae, and Bacillus cereus* as detailed by Mpeta *et al*. (2025).

2.2 Experiment media

In this experiment, synthetic wastewater at varying concentrations (1.5 mg/L, 3 mg/L and 6 mg/L) was used. Synthetic wastewater composed of mineral salt medium (MSM) prepared as described by Tendenedzai, Chirwa and Brink (2021) was supplemented with Au (III) in the form of $HAuCl_4$ to the experimental concentrations.

2.3 Analytical Methods

Au (III) concentration was measured periodically by Inductively Coupled Plasma Optical Emission spectrometry (ICP-OES) analytical Arcos model and atomic absorption spectroscopy (AAS) (Perkin Elmer A Analyst, Model AA400, CA, USA at 242.8 nm wavelength equipped with a 290 mA gold lamp) to track Au (III) reduction. Metal ion calibrations and QC followed established protocols. Biomass was monitored by measuring OD_{600} using the PerkinElmer Lambda 950 UV–VIS spectrophotometer (dual-beam technology).

2.4 Characterization of Gold Nanoparticles

After 24 h, cells and precipitates were collected by centrifugation. Formation of AuNPs was confirmed by imaging and spectroscopy. Scanning Electron Microscopy (SEM) coupled with Energy-Dispersive X-ray Spectroscopy (EDS), Zeiss Ultra Plus field emission model was used to observe particle morphology and elemental composition. X-ray Diffraction (XRD) Bruker D8 Advance model, patterns identified crystalline Au (0) (face-centered- cubic). Transmission Electron Microscopy (TEM) FEGTEM: Jeol 2100 (Peabody, MA, USA) model provided high-resolution images of particle size and shape.

2.5 Kinetic Experiments

Au (III) reduction assays were carried out at 35 °C, pH 7 (synthetic), sampling at various time intervals within a period of 18h. Batch reactors (250 mL amber plastic bottles) were inoculated with the consortium (grown overnight in TSB to reach stationary phase) and incubated aerobically at 35 ± 2 °C with shaking (100 rpm). Periodic samples were taken centrifuged at 9000 RPM in 5mins and supernatant sent for analysis. Remaining Au (III) was determined by ICP-OES/ AAS; Au (0) in solids by difference and imaging. Control flasks (abiotic and killed biomass) showed negligible Au (III) loss. The Monod model was first fitted followed by pseudo-first order (PFO) kinetic model to the Au (III) depletion data. Parameter estimation was performed using AQUASIM (a dynamic simulation software for aquatic systems). The best-fit model parameters (rate constants, affinity terms) were obtained by minimizing residuals (weighted least squares) with quality-of-fit assessed by R^2 and the best fitting model was selected.

3. Results and Discussions

3.1 Experimental Au (III) Reduction Efficiency

The consortium rapidly reduced Au (III) in the various concentrations of media (Figure 1). In synthetic wastewater (pH 7, 35°C), 87- 99% of Au (III) was removed within 18 h. (Figure 1).

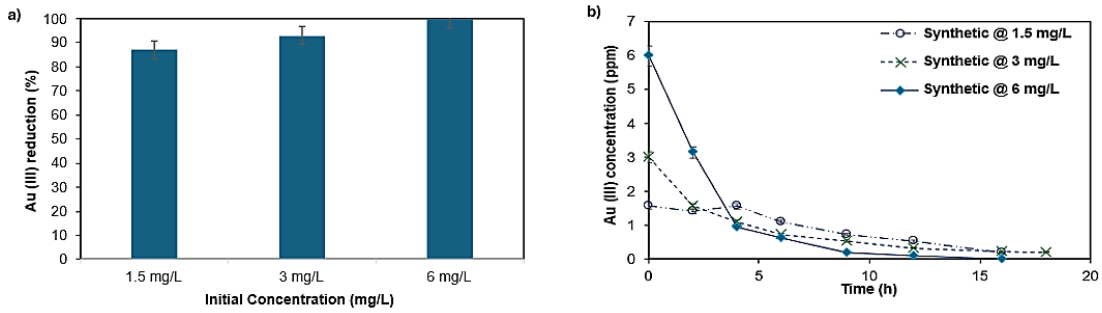

Figure 1: a) Au (III) percentage reduction in synthetic wastewater at varying concentrations (1.5, 3 and 6 mg/L) b) measured experimental data of Au (III) reduction over 18h period by bacteria consortium.

The bar graph demonstrates a strong positive correlation between initial Au (III) concentration and bioreduction efficiency by the bacterial consortium. The reduction efficiency increased progressively from approximately 87% at 1.5 mg/L to 93% at 3 mg/L, achieving nearly complete reduction (~99%) at 6 mg/L. Higher initial concentrations led to higher absolute reduction rates (more Au (III) removed per unit time in the early stages), but the residual concentration at the end is similar across all cases (~0.01–0.2 ppm). This indicates that the process has a limited capacity or equilibrium residual, independent of starting concentration.

This concentration-dependent behaviour is consistent with the reaction operating in the substrate-limited, first-order region of a saturation-type (Monod) kinetic model (Section 3.3). Reduction rate scales approximately linearly with the available Au (III) concentration, rather than reflecting saturation of the bacterial reducing enzymes (Chua et al., 2024; Contreras et al., 2025). Higher Au (III) concentrations may also stimulate enhanced bacterial reductase activity through substrate-induced metabolic activation (Mosquera-Romero et al., 2023). Lower concentrations result in substrate limitation that prevents complete reduction within the experimental timeframe. The fitted half-velocity constant (kc1 = 2830.36 mg/L, Table 1) is 470- to 1900-fold higher than the Au (III) concentrations tested (1.5-6 mg/L), confirming that the bacterial reductase system operates well below saturation across the full experimental range, consistent with first-order substrate dependence (Chua et al., 2024; Contreras et al., 2025). The consistently high reduction efficiency exceeding 85% across all tested concentrations indicates that the bacterial consortium remains effective over a broad concentration range, making it a versatile platform for diverse applications including bioremediation, gold recovery, and controlled biosynthesis of gold nanoparticles.

3.2 Experimental Kinetics

The decline appeared to follow pseudo-first-order or exponential across all concentrations, with the steepest initial drop at higher concentrations suggesting a concentration-dependent rate (Figure 1). The process approaches a similar low residual regardless of starting concentration (Figure 1b). This suggests a saturation effect or that the system is limited by reductant availability, surface sites, or equilibrium (Chua *et al.*, 2024).

3.3 Kinetic Modelling

In the present study, the bioreduction of Au (III) by bacterial consortium was evaluated at three different initial concentrations (6 mg/L, 3 mg/L, and 1.5 mg/L), and a kinetic model was developed to describe the process. The experimental data across all three concentrations exhibited a characteristic exponential decay pattern. Parameter estimation in AQUASIM was performed using a saturation (Monod-type) rate expression, Eq. (1a), which reduces to an apparent (pseudo-) first-order form under the experimental conditions tested here, as shown in Eq. (1a') and integrated in Eq. (1b):

$$\frac{-d[Au(III)]}{dt} = \frac{k_1[Au(III)]}{k_{c1}+[Au(III)]} \quad (1a)$$

Here k_1 (h^{-1}) is the maximum rate coefficient and kc_1 (mg/L) is the half-velocity (saturation) constant reported in Table 1. Because the Au (III) concentrations tested (1.5–6 mg/L) are 470- to 1900-fold lower than kc_1 (2830.36 mg/L), [Au(III)] ≪ kc_1 throughout the assay, and Eq. (1a) simplifies to the apparent (pseudo-) first-order form, with $k_{app} = k_1/kc_1$:

$$\frac{-d[Au(III)]}{dt} \approx -\frac{k_1}{k_{c1}}[Au(III)] = -k_{app}[Au(III)] \quad (1a')$$

Integrating Eq. (1a') between t = 0 and t gives the pseudo-first-order integrated form used to describe the exponential Au(III) decay observed experimentally:

$$[Au(III)]_t = [Au(III)]_0 e^{-k_{app}t} \quad (1b)$$

The Monod model performance varied with initial Au (III) concentration, showing excellent predictive capability at higher substrate concentrations. At 6 mg/L Au (III), the model exhibited a good fit with an estimated R^2 value of approximately 0.913. It showed both the rapid initial reduction phase (0-5 hours) and the subsequent slower reduction kinetics through completion at approximately 15 hours. At 3 mg/L, Au (III), the model had a good fit with an estimated R^2 of 0.977, closely tracking the experimental data with only minor deviations observed between 5-10 hours. However, at the lowest concentration of 1.5 ppm Au (III), the model fit decreased somewhat with an estimated R^2 of 0.586. It showed noticeably greater scatter in the experimental measurements, particularly during the early reduction phase (2-8 hours). This decline in model performance at lower concentrations is typical of biological systems and inherent biological variability when approaching detection limits.

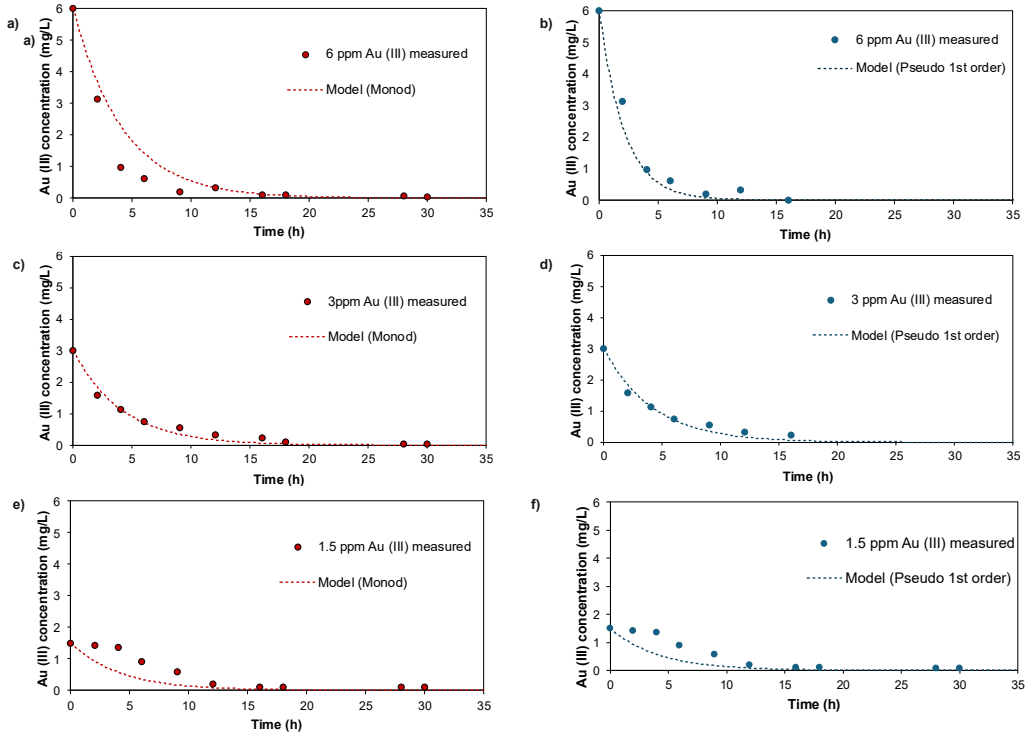

Figure 2: Monod model fit (a, c, e) and pseudo first order kinetics (b, d, f) fitted to measured 1.5 mg/L, 3 mg/L and 6 mg/L Au (III) reduction

The underlying rate expression, Eq. (1a), is a saturation (Monod-type) model in which reduction rate depends on both a maximum rate coefficient (k_1) and a half-velocity constant (kc_1). The kc_1 (2830.36 mg/L) greatly exceeds the Au(III) concentrations tested (1.5-6 mg/L), the model operates in its linear, substrate-limited region and is well-approximated by the pseudo-first-order form, Eq. (1a') and (1b). Using the R^2, the Pseudo first order provides a better fit than the Monod model for Au (III) bioreduction by the consortium across the concentration range relevant to mine wastewater (1.5 mg/L= 0.726; 3 mg/L= 0.969 and 6 mg/L= 0.968).The concentration-dependent reduction rates, where higher initial concentrations showed faster absolute reduction while maintaining the same fundamental exponential-decay pattern, further support this pseudo-first-order behaviour. The rate of Au (III) reduction is directly proportional to the remaining substrate concentration at any given time, which is characteristic of an enzyme-mediated process operating below saturation. The good overall agreement between model predictions and experimental observations, particularly at environmentally and industrially relevant concentrations (3-6 mg/L), demonstrates that this pseudo-first-order kinetic model provides a robust framework for understanding Au (III) bioreduction kinetics. Such capability is essential for process optimization, scale-up design, and practical applications in bioremediation and gold nanoparticle biosynthesis.

The best-fit kinetic parameters obtained from parameter estimation (the maximum rate coefficient k_1 and the half-velocity constant kc_1 are summarised in Table 1.

Table 1: Model estimated parameters

Parameter	Model estimated value	Units
Reaction rate coefficient (k1)	681.96	h^{-1}
Half velocity concentration (kc1)	2830.356	mg/L

The kinetic modeling confirms that the reduction is rapid and likely enzyme mediated. Applying $k_{app} = k_1/kc_1 = 681.96/2830.36 = 0.24\ h^{-1}$ (Eq. 1a') gives an effective pseudo-first-order half-life of ≈2.9 (from ln2/k) h and a predicted time to 99% Au (III) removal of ≈19 h, consistent with the 15-18 h required for complete reduction observed experimentally (Section 3.1). This confirms that k_1 in Table 1 is a maximum rate coefficient of the saturation kinetic expression rather than a first-order rate constant, and that the apparent first-order rate constant relevant to the timescale of the process is k_{app}, not k_1. Beyond confirming rapid Au (III) reduction, this study extends the prior characterisation of the same consortium (Mpeta *et al.*, 2025) by providing, for the first time, a kinetic model for its Au (III) reduction behaviour. Compared with the reductase-based mechanisms reported for single strains such as *Erwinia* sp. IMH (Wang *et al.*, 2022) and engineered reductase variants (Chua *et al.*, 2024), the mixed consortium used here derives its performance from metabolic complementarity and resource partitioning among four indigenous strains, which may confer greater robustness and adaptability to the variable metal loads and co-contaminants typical of real mine effluents than single-strain systems (Mpeta *et al.*, 2025). Relative to conventional gold recovery routes such as cyanide or thiourea leaching (Malarkodi *et al.*, 2013), which require harsh reagents and generate toxic secondary waste, the biologically driven process described here operates under mild, near-neutral conditions (pH 7, 35°C) while achieving comparable removal efficiencies (87-99%). Studies with fitted kinetic parameters for microbial Au(III) bioreduction are not there, so a direct numerical comparison was not possible. Closest precedents are AQUASIM-based Monod models for Cr(VI) (Igboamalu and Chirwa, 2016) and Se(VI) (Tendenedzai *et al.*, 2021) reduction. It offers potentially safer and more sustainable alternative, even though one so far has been demonstrated only at laboratory batch scale.

3.4 Nanoparticle Characterization

At the different concentrations, visual colour change during reduction was noticed. The formed nanoparticles were purple/red as Au (0) formed as shown in figure 2a and 2b. TEM images (Figure 3) showed abundant electron-dense particles inside of cells and extracellular aggregates.

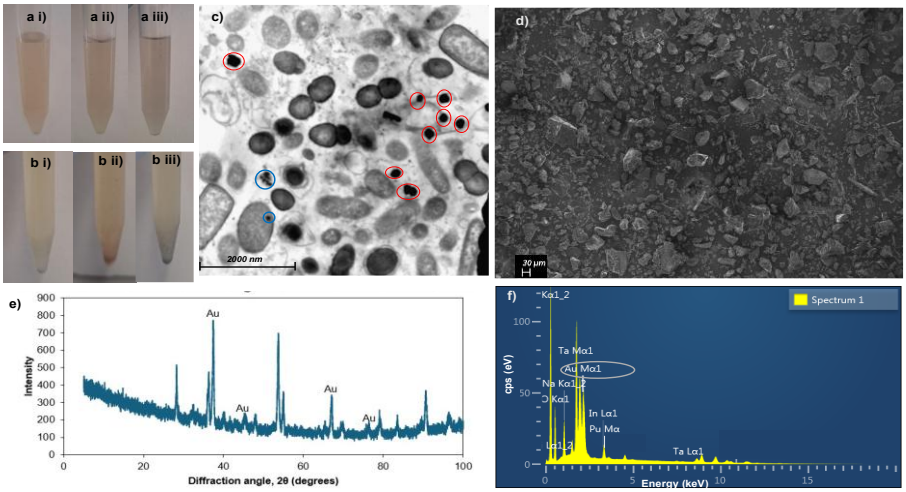

Figure 3: a) Samples showing visual differences and Au nanoparticle formation between 1st hour; b) after 18 hours at concentrations of i) 1.5mg/L, ii) 3mg/L and iii) 6mg/L; c) TEM images showing nanoparticle reduction extracellular (red circles) and intracellular formation (blue circles); d) Dried nanoparticles SEM image and accompanying; e) XRD and f) EDS profile

SEM with EDS spectra (figure 3d and f) confirmed strong Au peaks at ~2.5 keV. XRD of dried biosynthesised nanoparticles sample revealed distinct diffraction peaks at 2θ ≈ 38°, 44°, 64° and 78° corresponding to Au (0) face-centered cubic (111), (200), (220) planes.

4. Conclusion

This study presents a comprehensive kinetic analysis of microbial Au (III) bioreduction by a tailored bacterial consortium. 87% to near complete Au (III) reduction was achieved in 18 h under aerobic conditions. Intracellular

and extracellular formation of Au (0) nanoparticles confirmed by SEM-EDS, XRD, and TEM. Successful modelling of reduction kinetics using pseudo-first-order models ($0.726 > R^2 > 0.97$), implemented in AQUASIM for predictive simulation. These results, obtained under controlled batch conditions using synthetic wastewater, provide a promising basis for future bioreactor design studies. Future work will focus on validating Au (III) reduction in real mine wastewater, more rigorous statistical comparison between the two models and integrating with other resource recovery operations.

Conflict of Interest: None declared.

References

Abd El-Aziz, M., Badr, Y., Mahmoud, M. A., Husseiny, M. I., Badr, Y., Mahmoud, M. A., Abd El-Aziz, M., Badr, Y., & Mahmoud, M. A., 2007, Biosynthesis of gold nanoparticles using Pseudomonas aeruginosa. AIP Conference Proceedings, 888(June 2016), 177–181. https://doi.org/10.1063/1.2711108

Chua, J. P. S., Rajasabhai, R., Teo, W. Z., Xue, B., & Yew, W. S., 2024, Engineering a Metal Reductase for the Bioremediation of Anthropogenic Electronic Wastes: From Hg(II) to Au(III) and Ag(I) Enzymatic Reduction. JACS Au, 4(6), 2335–2342. https://doi.org/10.1021/jacsau.4c00297

Contreras, F., Rivero, K., Rivas-Pardo, J. A., Liendo, F., Segura, R., Neira, N., Arenas-Salinas, M., Cortez-San Martín, M., Arenas, F., Mosquera-Romero, S., Anaya-Garzon, J., Garcia-Timermans, C., Van Dorpe, J., Hoorens, A., Commenges-Bernole, N., Verbeken, K., Rabaey, K., & Varia, J., 2025, Combined Gold Recovery and Nanoparticle Synthesis in Microbial Systems Using Fractional Factorial Design. International Journal of Molecular Sciences, 26(5), 1–16. https://doi.org/10.3390/nano13010083

Guo, X., & Wang, J., 2025, Kinetic models in environmental biotechnological processes: Origin, derivation and applications. Chemosphere, 374(February), 144217. https://doi.org/10.1016/j.chemosphere.2025.144217

Huang, X., El-Sayed, I. H., Yi, X., & El-Sayed, M. A., 2005, Gold nanoparticles: Catalyst for the oxidation of NADH to NAD+. Journal of Photochemistry and Photobiology B: Biology, 81(2), 76–83. https://doi.org/10.1016/j.jphotobiol.2005.05.010

Igboamalu, T. E., & Chirwa, E. M. N., 2016, Kinetic study of Cr(VI) reduction in an indigenous mixed culture of bacteria in the presence of As (III). Chemical Engineering Transactions, 49(VI), 439–444. https://doi.org/10.3303/CET1649074

Jin, Q., 2023, Building microbial kinetic models for environmental application: A theoretical perspective. Applied Geochemistry, 158(January), 105782. https://doi.org/10.1016/j.apgeochem.2023.105782

Lengke, M. F., Ravel, B., Fleet, M. E., Wanger, G., Gordon, R. A., & Southam, G., 2007, Precipitation of gold by the reaction of aqueous gold (III) chloride with cyanobacteria at 25-80°C - Studied by X-ray absorption spectroscopy. Canadian Journal of Chemistry, 85(10), 651–659. https://doi.org/10.1139/V07-024

Luo, C. H., Shanmugam, V., & Yeh, C. S., 2015, Nanoparticle biosynthesis using unicellular and subcellular supports. NPG Asia Materials, 7(8). https://doi.org/10.1038/am.2015.90

Malarkodi, C., Rajeshkumar, S., Vanaja, M., Paulkumar, K., Gnanajobitha, G., & Annadurai, G., 2013, Eco-friendly synthesis and characterization of gold nanoparticles using Klebsiella pneumoniae. Journal Of Nanostructure in Chemistry, 3(30), 1–7. https://doi.org/http://www.jnanochem.com/content/3/1/30

Mata, Y. N., Torres, E., Blázquez, M. L., Ballester, A., González, F., & Muñoz, J. A., 2009, Gold(III) biosorption and bioreduction with the brown alga Fucus vesiculosus. Journal of Hazardous Materials, 166(2–3), 612–618. https://doi.org/10.1016/j.jhazmat.2008.11.064

Mosquera-Romero, S., Anaya-Garzon, J., Garcia-Timermans, C., Van Dorpe, J., Hoorens, A., Commenges-Bernole, N., Verbeken, K., Rabaey, K., & Varia, J., 2023, Combined Gold Recovery and Nanoparticle Synthesis in Microbial Systems Using Fractional Factorial Design. Nanomaterials, 13(1), 1–16. https://doi.org/10.3390/nano13010083

Mpeta, M., Tendenedzai, J. T., Tichapondwa, S. M., & Chirwa, E. M. N., 2025, Performance evaluation of gold (III) bio-reduction by bacterial strains and a consortium isolated from gold mine effluent. Minerals Engineering Journal, 235(June 2025), 0–11. https://doi.org/https://doi.org/10.1016/j.mineng.2025.109797

Tendenedzai, J. T., Chirwa, E. M. N., & Brink, H. G., 2021, Performance evaluation of selenite (SeO32−) reduction by Enterococcus spp. Catalysts, 11(9). https://doi.org/10.3390/catal11091024

Wang, L., Yan, L., Ye, L., Chen, J., Li, Y., Zhang, Q., & Jing, C., 2022, Identification and Characterization of a Au(III) Reductase from Erwinia sp. IMH. JACS Au, 2(6), 1435–1442. https://doi.org/10.1021/jacsau.2c00170

Wiesemann, N., Bütof, L., Herzberg, M., Hause, G., Berthold, L., Etschmann, B., Brugger, J., Martinez-Criado, G., Dobritzsch, D., Baginsky, S., Reith, F., & Nies, D. H., 2017, Synergistic toxicity of copper and gold compounds in Cupriavidus metallidurans. Applied and Environmental Microbiology, 83(23). https://doi.org/10.1128/AEM.01679-17